DENDROGEOMORPHIC EVIDENCE OF FREQUENT MASS MOVEMENT USING REACTION WOOD IN BLACK SPRUCE: ALASKA HIGHWAY MILEPOST 1267, NORTHWAY JUNCTION, ALASKA

Alexander K. Stewart, Catherine E. Heinrich, and Trent D. Hubbard

Report of Investigations 2017-7

Split black spruce trunk resulting from extensional mass movement, Northway Junction, Alaska. Photo by Alexander K. Stewart.

STATE OF ALASKA | DEPARTMENT OF NATURAL RESOURCES | DIVISION OF GEOLOGICAL & GEOPHYSICAL SURVEYS

DENDROGEOMORPHIC EVIDENCE OF FREQUENT MASS MOVEMENT USING REACTION WOOD IN BLACK SPRUCE: ALASKA HIGHWAY MILEPOST 1267, NORTHWAY JUNCTION, ALASKA

Alexander K. Stewart, Catherine E. Heinrich, and Trent D. Hubbard

Report of Investigations 2017-7

State of Alaska
Department of Natural Resources
Division of Geological & Geophysical Surveys

STATE OF ALASKA
Bill Walker, *Governor*

DEPARTMENT OF NATURAL RESOURCES
Andrew T. Mack, *Commissioner*

DIVISION OF GEOLOGICAL & GEOPHYSICAL SURVEYS
Steve Masterman, *State Geologist and Director*

Publications produced by the Division of Geological & Geophysical Surveys (DGGS) are available for free download from the DGGS website (dggs.alaska.gov). Publications on hard-copy or digital media can be examined or purchased in the Fairbanks office:

Alaska Division of Geological & Geophysical Surveys
3354 College Rd., Fairbanks, Alaska 99709-3707
Phone: (907) 451-5010 Fax (907) 451-5050
dggspubs@alaska.gov | dggs.alaska.gov

DGGS publications are also available at:

Alaska State Library, Historical Collections & Talking Book Center
395 Whittier Street
Juneau, Alaska 99811

Alaska Resource Library and Information Services
3150 C Street, Suite 100
Anchorage, Alaska 99503-3982

CONTENTS

FIGURES

TABLES

DENDROGEOMORPHIC EVIDENCE OF FREQUENT MASS MOVEMENT USING REACTION WOOD IN BLACK SPRUCE: ALASKA HIGHWAY MILEPOST 1267, NORTHWAY JUNCTION, ALASKA

Alexander K. Stewart[1], Catherine E. Heinrich[2], and Trent D. Hubbard[3]

INTRODUCTION

In preparation for construction of proposed natural-gas pipelines, the Alaska Division of Geological & Geophysical Surveys (DGGS) has been investigating geologic hazards along several proposed corridors, including the Alaska Highway between Delta Junction and the Canada border. The Alaska Highway is the only major road connecting Alaska to Canada and the contiguous United States and thus understanding slope movement is important, not only for potential pipeline routing, but also because it will help those making permitting, maintenance, and planning decisions along this important transportation corridor.

DGGS identified three large, retrogressive landslides expanding headward toward the Alaska Highway from the southwest-facing bluffs of the Chisana River near Northway Junction, Alaska, between Alaska Highway mileposts (AMP) 1265 and 1267. These slope failures were probably initiated by stream erosion along the margin of the Chisana River floodplain, and are dominated by complex slumping of blocks of thawing, perennially frozen, sandy silts (Reger and others, 2012a). The large failure near AMP 1267 seriously affected the Alaska Highway and in 2004 required revising the highway alignment (fig. 1). Cracks that developed in pavement emplaced in summer 2008 and later and in adjacent fill along the Alaska Highway near AMP 1267 demonstrate continuing northward expansion of the landslide along this remote international corridor (fig. 2).

Generally, low-volume roads (LVR; <1,000 cars/day) such as the Alaska Highway (AH) are economically and socially important to the communities they serve (and the larger international relations associated with the cross-border aspect) (Bowman, 2015). Because the more than 2,700-km-long AH was built very rapidly (in 1942 in less than one year) and through austere, wild environments, general design and maintenance planning were poorly developed and/or implemented (DoD, 1944; Bowman, 2015). Aggravating the LVR issue is the overall remoteness of any section of the AH and its association with underlying permafrost which, with projected warming in this region of Alaska (as seen in the NOAA Northway Airport weather station PAOR; CLIMOD, 2016), will be an increasing problem (Larsen and others, 2008). Relatively few efforts have been made to understand the rates and chronology of mass-movement events along remote, LVR corridors; however, the few attempts to understand these common events are beginning to help engineers, planners, and communities better prepare for this eventuality (Bowman, 2015).

BACKGROUND

The Alaska Highway, "the key which unlocked the treasure chest of Alaska" (DoD, 1944), was originally constructed in cooperation with Canada as a military winter, pioneer road with temporary bridges that connected the contiguous U.S. to Alaska (DoD, 1944). It was hastily completed from March through November 1942 to support the strategic defense of Alaska and North America during World War II (DoD, 1944) and was not opened to the public until 1948. After the first winter's use (1942–1943), the nascent AH was more efficiently rerouted, straightened, and surfaced with gravel, leading to an all-weather road that was completed in October 1943 (DoD, 1944). Despite these efforts to improve the route, it has required occasional realignments and significant maintenance ever since its initial construction. Individual sections along the route continue to sustain site-specific issues associated with improper engineering, permafrost (such as thawing; see Wallace, 1948), and/or general mass movement, among others.

[1]Department of Geology, St. Lawrence University, 23 Romoda Drive, Canton, NY 13617; astewart@stlawu.edu
[2]Department of Geology, St. Lawrence University (graduated, 2015).
[3]Alaska Division of Geological & Geophysical Surveys, 3354 College Road, Fairbanks, AK 99709-3707; trent.hubbard@alaska.gov

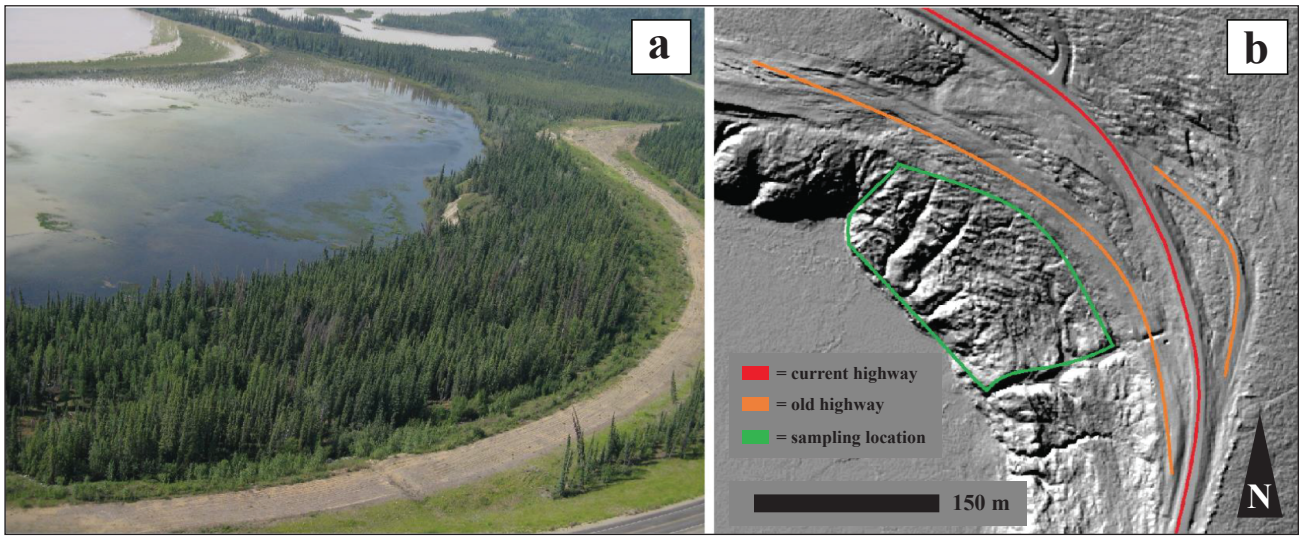

Figure 1. Sampling site along the Alaska Highway at milepost 1267. (a) Oblique aerial photograph facing westerly; and (b) lidar image with roads and sampling area. From Hubbard and others (2011).

Figure 2. Google Earth Street View (October 2011) facing west-northwest along the Alaska Highway near milepost 1267. Notice the recently flagged and patched roadway in the east-bound lane; the first break in the tree line to the south of the roadway is the old, pre-2004 roadway.

One particular section of the highway, centered near Northway Junction, Alaska, has recently undergone extensive engineering analyses, rerouting, and multiple repavings. In 1984, an engineering and soils report was completed to assess availability of crushed materials for local roadwork (Brazo, 1984) and was followed by a geotechnical report of the original, road-altering, mass-movement event at AMP 1267–68, in preparation for a realignment (Kinney, 1993) and again in 1994 for additional resource allocation for the area (Bennett, 1994). Since the 2004 northward realignment of the road after the mass-movement event, continued road movement has required repairs along this new section in most of the years since (Reger and others, 2012a; Jeff Currey [DOT&PF], written commun., 2014). Despite the best engineering efforts, as of 2004 this section of the AH is still undergoing mass-movement-related roadway issues and will likely need significant attention in the near future (fig. 2).

LOCATION AND GEOLOGICAL SETTING

The focus of this study is an active, retrogressive landslide complex expanding toward the Alaska Highway near Northway Junction, Alaska, at approximately 63.046°N, 141.829°W (fig. 3), in the Tetlin National Wildlife Refuge. These three large, retrogressive mass movements are at the southern margin of the Yukon–Tanana Upland adjacent to the Northway–Tanacross Lowland, which is part of the Alaska Boreal Interior (taiga) and, more specifically, the Interior Bottomlands (Wahrhaftig, 1965; Wiken and others, 2011). The Northway–Tanacross Lowland separates the Yukon–Tanana Upland from the easternmost Alaska Range. Our approximately 4-hectare sampling site was on the landslide complex on the southwestern side of the Alaska Highway (AH) 42 km west of the Canada border (figs. 1 and 3).

The low, rolling bedrock hills of the Yukon–Tanana Upland are part of the Yukon–Tanana terrane and generally consist of Devonian- to Cretaceous-aged metamorphic and metaigneous rocks, including amphibolite phyllite, schist, gneiss, quartzite, marble argillite, greenstone metasandstone and metaconglomerate, and metagabbro, with Mesozoic to Tertiary granitic intrusions (Kinney, 1993; Wilson and others, 2015; Solie and others, in review.

Surficial-geologic materials along the southern margins of the Yukon–Tanana Upland along the Alaska Highway southeast of Tok consist of widespread stabilized aeolian sand dunes and blankets overlain by thin loess. Retransported sand and loess form complex, perennially frozen valley fills (Reger and others, 2012b; in press). In and above surficial deposits several Quaternary tephras associated with eruptions from the

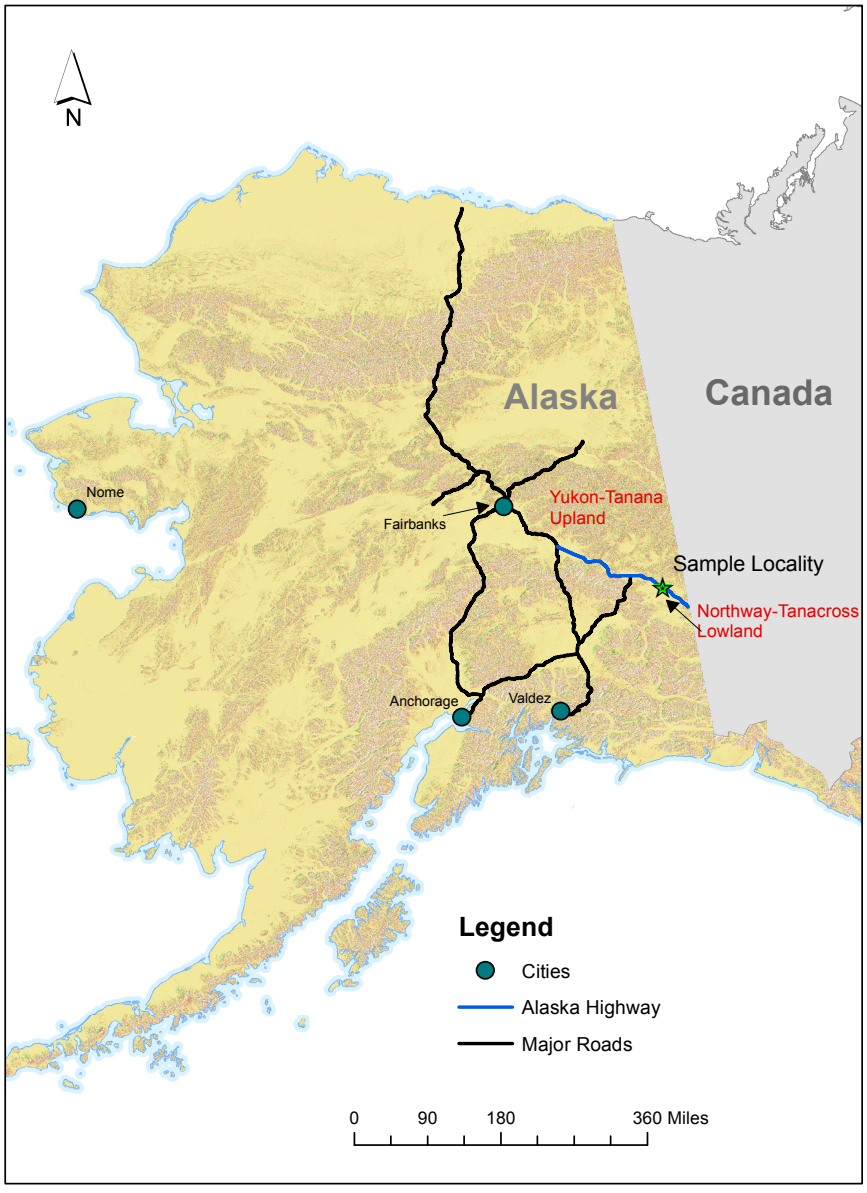

Figure 3. Shaded relief map of Alaska with sampling site location marked with star.

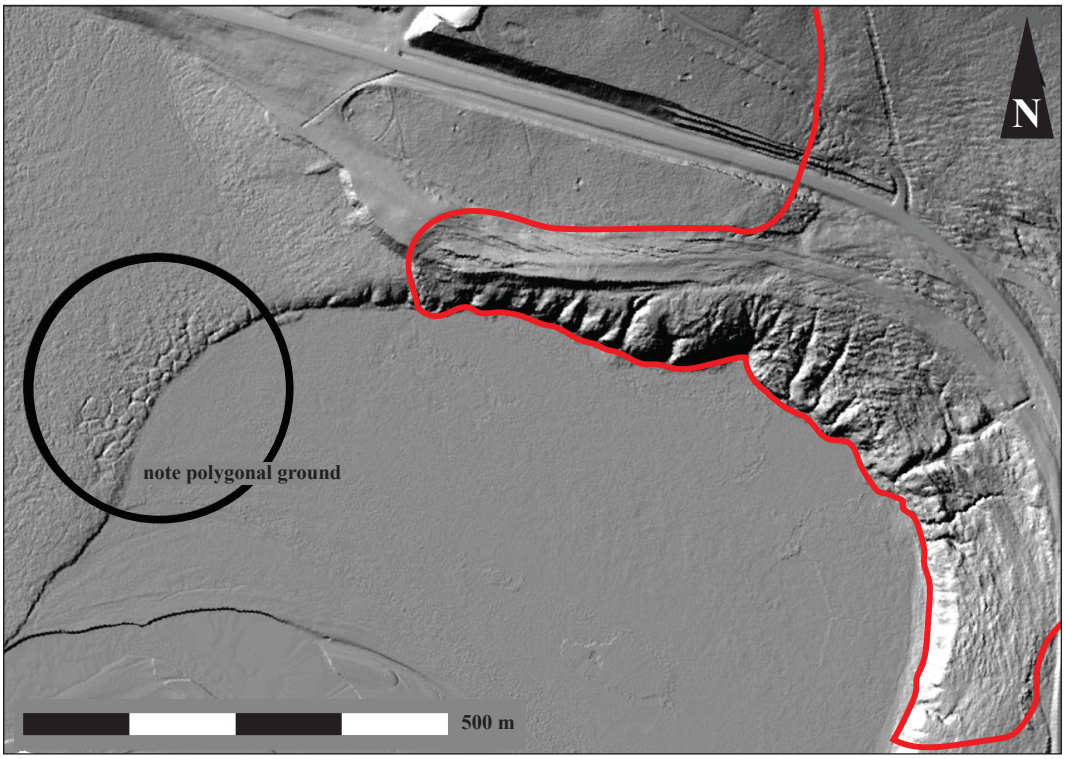

Figure 4. Lidar image of the sampling site with the red line around the approximate area of disturbance and the black circle showing adjacent polygonal ground. From Hubbard and others (2011).

Wrangell and St. Elias mountains have been identified, including the White River Ash, Old Crow, and Sheep Creek tephras near AMP 1284 (Schaefer, 2002). The Northway–Tanacross Lowland consists of widespread areas of alluvial deposits, including active and inactive channel deposits, as well as abandoned floodplain terrace deposits (Reger and others, 2012b; in press). Stabilized sand dunes occupy many of the higher stream terraces, a result of north-blowing katabatic winds.

At a regional scale the Northway–Tanacross Lowland is in the zone of discontinuous permafrost (Jorgenson and others, 2008). The area is characterized by extensive peat lands, with patterned ground features being common (CEC, 1997; fig. 4). Recent investigations by Reger and others (2012a) reveal that lowland permafrost generally has low to moderate ice content on older terraces and abandoned floodplains with extensive scrublands. These investigations also indicate that permafrost is sporadic in sediments on inactive and abandoned floodplains along active channels and in scrublands on low fluvial terraces, where surface water bodies are numerous, scattered, small, and shallow. Many of the thaw lakes, present in fine-grained sediment, typically exhibit circular to complex, locally scalloped shorelines, are 1.5 to 3 m deep, and have fairly flat bottoms (Wallace, 1948; Reger and others, in review).

In the southern Yukon–Tanana Upland, permafrost is more complexly distributed because of local differences in topographic relief, aspect, vegetation cover, and other factors, which have combined effects on permafrost distribution (Jorgenson and others, 2001; Shur and Jorgenson, 2007; Pastick and others, 2014, 2015). Jorgenson and others (2008) indicate that permafrost in the southern Yukon–Tanana Upland is discontinuous at a regional scale; however, investigations by Reger and others (in press) indicate that there can be localized areas of continuous permafrost. Permafrost is complexly distributed in the region because of local differences in topographic relief in zones conducive to permafrost preservation. In the study area, we observe sporadic or discontinuous permafrost of high-ice content in thick valley fills. In thin fills in upper drainages permafrost is more discontinuous with low to moderate ice content. Relatively warm, south-facing bedrock slopes are generally unfrozen, whereas ridge crests and upper eastern and western slopes are typically discontinuously frozen with low ice content.

ECOREGION (GALLANT AND OTHERS, 1995)

The Northway Junction area is part of the Interior Bottomlands ecoregion (Wahrhaftig, 1965; Wiken and others, 2011). This region is characterized by a continental climate with temperatures usually remaining above freezing through the summer (June through August), though they may dip below freezing during this time. This region comprises flat to nearly flat bottomlands along larger rivers of Interior Alaska. The bottomlands

are dotted with thaw and oxbow lakes with soils poorly drained and shallow and generally affected by permafrost. Predominant vegetation communities include forests dominated by spruce and hardwood species, tall shrub thickets, and wetlands. Needleleaf, broadleaf, and mixed forest stands populate a variety of sites in the Interior Bottomlands ecoregion. Tall scrub communities form thickets on floodplains. Scrublands, which have open to closed canopies of low shrubs dominated by dwarf birch and ericaceous shrubs, include black spruce and larch and are one of the most widespread ecosystems in Alaska (Jorgenson and others, 2001). The wettest sites support a variety of wetland communities, such as low scrub bogs, wet graminoid herbaceous meadows, and wet forb herbaceous marshes and meadows. Needleleaf forests are dominated by white spruce (*Picea glauca*) and/or black spruce (*Picea mariana*). Closed stands of white spruce occupy young river terraces where soil drainage is good, with closed stands of black spruce existing on well-drained to poorly drained floodplain soils (Gallant and others, 1995).

DENDROGEOMORPHOLOGY

Dendrochronology is the dating and study of annual growth layers, or tree rings, in woody trees and shrubs. It is important not only for its ability to determine the age of a tree, but also because it can be used to determine, with one-year precision, the dates of a variety of environmental events. Because of its one-year accuracy, the science of dendrochronology has expanded beyond typical forestry uses (such as stand age) to many diverse studies involving trees (for example, Speer, 2010; Stoffel and others, 2010). Dendrogeomorphology, used in this study, is the analysis of geomorphologic processes using dendrochronological techniques, and was first introduced by Jouka Alestalo (1971). The application of dendrochronology to geomorphic processes can provide a temporal and spatial aspect to the practical problems surrounding mass movement (Stoffel and others, 2013). The annual resolution of the tree-ring record preserves valuable archives of past geomorphic processes on timescales from decades to centuries (Stoffel and Corona, 2014). Many of these processes are significant natural hazards; understanding their distribution, timing, and controls provides crucial information that can assist in the prediction, mitigation, and defense against these hazards and their effects on society.

PICEA MARIANA (BLACK SPRUCE)

Picea mariana (black spruce, bog spruce, swamp spruce) is an abundant conifer of northern North America. Its wood is yellow–white in color, relatively light in weight, and strong (Viereck and Johnston, 1990). Black spruce trees are present on a wide range of sites, from wet lowlands to drier uplands, and in a variety of soils. The species is most common on poorly drained sites underlain with permafrost and is common throughout much of Alaska from the Brooks Range south (fig. 5). Ericaceous shrubs commonly grow in black spruce understories, with mosses and lichens in ground layers. Additionally, black spruce is important in other boreal mixed-conifer and conifer-hardwood communities. It is primarily a boreal species, although its distribution extends south into the Great Lakes and Northeast regions of the United States (fig. 5). Climate warming is apparently favoring expansion of black spruce's distribution in the north (Chapin and others, 2010; Fryer, 2014a) and shrinkage in the south (Hogg, 1994; Fryer, 2014a). Black spruce is an abundant and hearty species in the poorly drained, acidic soils of the Interior Bottomlands and was the primary tree species at our selection site.

METHODS

Mass movement can cause responses in tree growth ranging from obvious trunk curvature and/or scarring to changes in wood anatomy (for example, reaction wood) (Shroder, 1978). Growth-ring disturbances due to tilting are usually in the form of reaction wood (Shroder, 1978; Owczarek, 2005), where individual rings become considerably wider and slightly darker in appearance compared to the upslope side as the tree puts on structural mass to correct its posture (Warensjö and Rune, 2004; Carrara and O'Neill, 2010) (figs. 6 and 7). In conifer trees, tilting events cause stem deformation (Benninghoff, 1950) known to inhibit the growth of the terminal shoot because of initiation of reaction wood (compression wood in conifers) growth on the lower side of the stem (Cremer, 1998; Carrara and O'Neill, 2010). "It is formed by the cambium (or cambial derivatives) of the lower side of inclined stems and branches, where it expands in place, thereby tending to right the former and maintain (restore) the inherent angle of the latter" (Westing, 1965, p. 382). Reaction-wood growth in the trunk is most clearly visible in the basal segment of the tree, to which the center of gravity has been moved through the inclination of the stem axis (Mattheck, 1993). The initial year of reaction wood growth is usually during the event-year's remaining ring growth or the following year (if the tilting occurred during non-growth periods) (Carrara and O'Neill, 2010); however, in at least one case (Carrara, 2002) reaction-

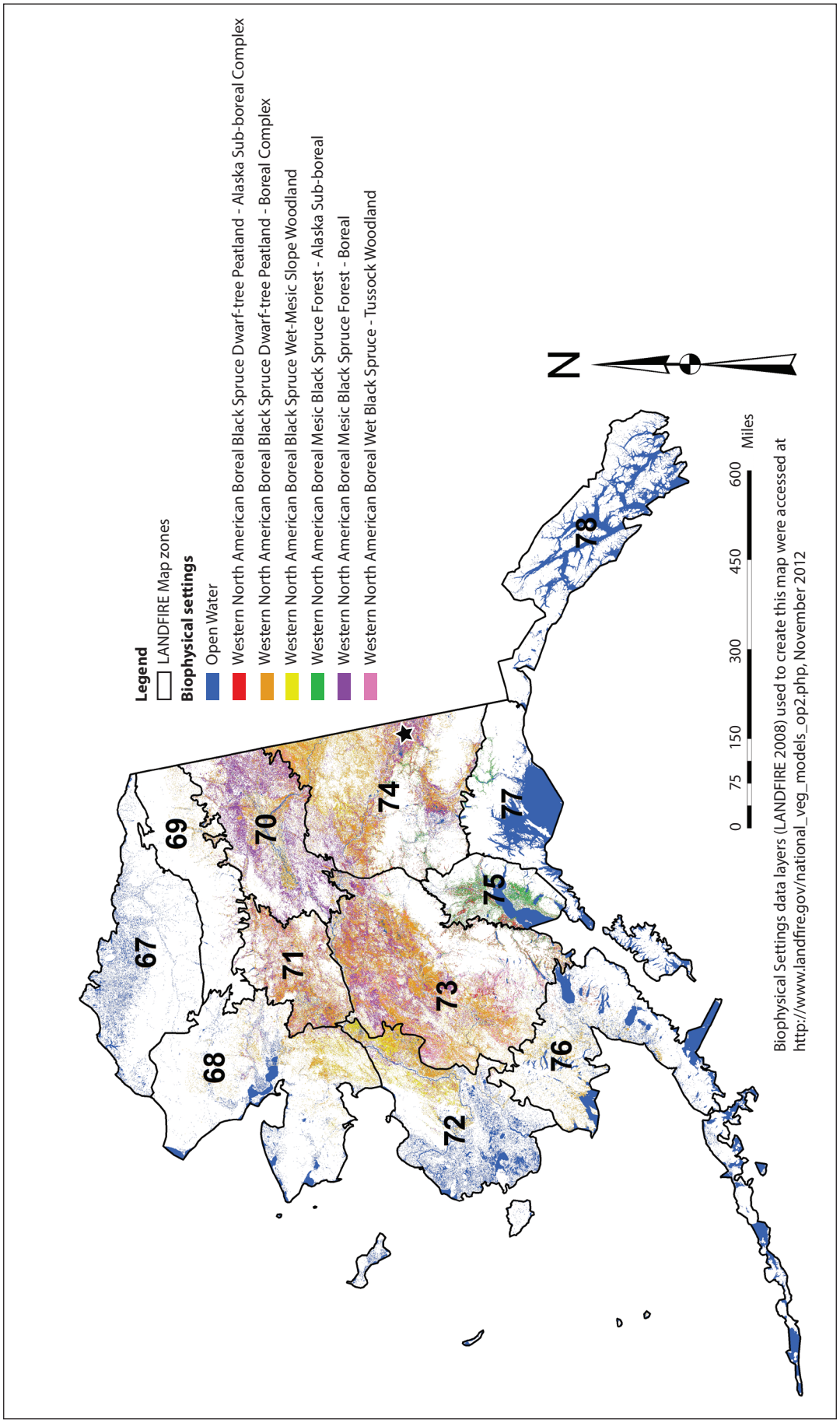

Figure 5. Distribution map for Alaska black spruce (*Picea mariana*) (modified from Fryer, 2014b). Numbers indicate LANDFIRE map zones (https://www.landfire.gov/NationalProductDescriptions20.php). Black star is sampling location.

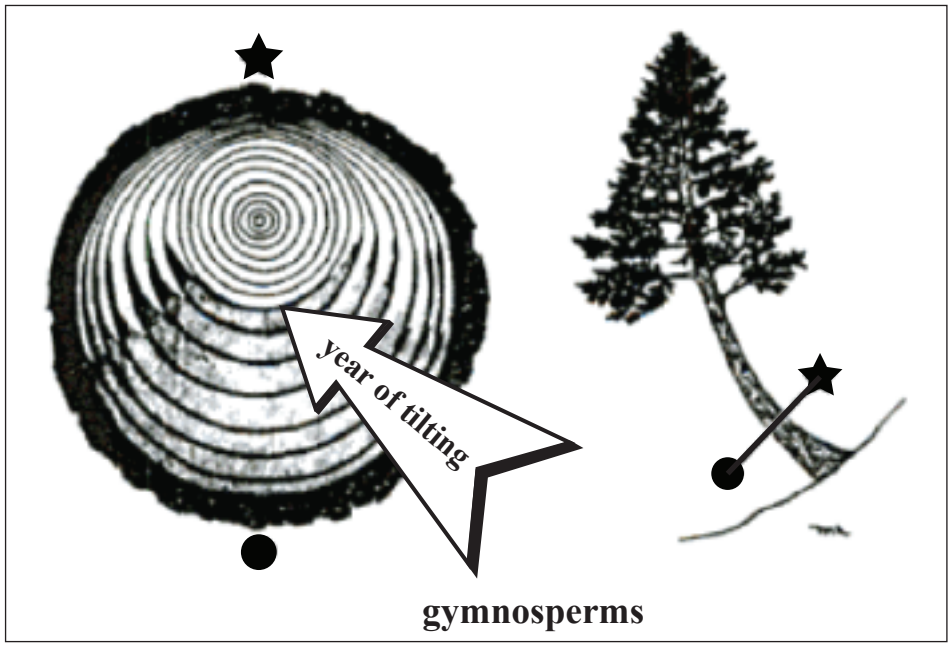

Figure 6. Schematic representation of altered ring growth as a result of tree tilting, with reaction wood (compression wood in conifers [gymnosperms]) growing on the lower side of the tilt. Dot and star show orientation of cross section. Modified from Fritts (1976).

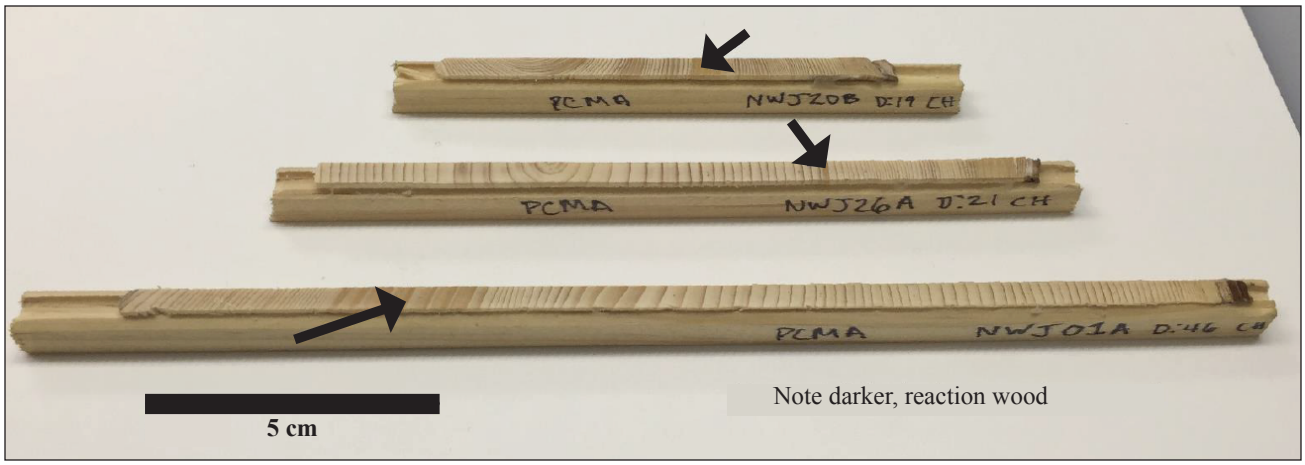

Figure 7. Three samples highlighting reaction wood in three separate trees. Arrows point out sections of reaction wood (darker than surrounding sections).

wood onset was delayed for several years with recovery lasting from three to nine years after the tilting event. Reaction-wood analysis is key to unlocking the spatial and chronological distribution of instability at a site. Our working assumption is that reaction wood begins growing just after a tilting event (for example, Westing, 1965; Cremer, 1998).

TREE SAMPLING AND CORE PREPARATION

Onsite tree selection was preferential with only visibly tilted trees being sampled (fig. 8). Using a Swedish increment borer, we collected two samples each from 30 black spruce trees (n=60). One core was taken through the reaction wood (core a), or from the direction of tree tilt, and another was taken at a 90° angle to the first (core b), as suggested by Fantucci and McCord (1995) and Stoffel (written commun.). At each location we recorded the GPS coordinates, tree height, diameter at breast height (DBH), height at which the sample was taken, elevation, direction and angle of the tilt, direction and angle of slope (if any), the crown density, and the average thaw depth of the permafrost, as well as additional notes such as line drawings of tree-trunk long-axis form (table 1). Thaw depth (as of June 1, 2014) was calculated as the mean of three depth measurements taken using a frost probe, equally spaced around the tree (120° offset) and 1.2 m away from the trunk. After the tree borings were removed from the increment borer they were stored in paper straws, labeled, and transported back to the tree-ring laboratory at St. Lawrence University, where dried cores were mounted with Elmer's glue to labeled wooden mounts. Cores were sanded with progressively finer sand paper, from coarse, 120-grit paper

Table 1. Summary of project data. Tree NWJ09 and samples 13a and 30b were removed due to poor sample quality.

Tree	Height of tree (m)	Elevation (m)	DBH (cm)	Height of sample (m)	Direction of tilt (Deg)	Angle of tilt (deg.)	direction of slope (deg.)	angle of slope (deg.)	avg ALD (cm)	crown density	Age (minimum)
01	24.8	560	46	1.2	342	6	200	5	14.6	high	133
02	17	564	38.5	1	320	5	250	8	18.3	avg-high	127
03	11.8	560	41	1.2	155	30	235	7	18.3	avg	138
04	11.2	559	19	1.2	85	25	175	5	73.3	avg	71
05	19.6	556	49	0.9	260	20	190	5	50.6	high	110
06	25.4	555	33	1	255	13	205	2.5	50	avg	107
07	26	557	41	1.2	65	13	150	10	21.6	avg	96
08	29.2	554	42	1.3	65	11	220	12	15.6	avg - low	194
10	14.2	546	24	1	215	22	220	20	25	avg-high	50
11	22.4	546	36.5	1.2	280	16	255	15	26	avg	101
12	26.6	552	32	1.3	20	12	265	10	19	avg	126
13	18.4	550	35	1.3	125	15	125	15	13	avg	162
14	19.4	561	28	1.1	115	10	265	15	16.6	low	75
15	10.2	567	23	1.3	30	18	160	7.5	21.3	low to very low	144
16	18.2	549	25	1.4	20	15	255	12	10.6	low	80
17	17.8	557	22	1	70	5	195	15	15	low	164
18	22.8	552	46	1.5	12	14	190	15	19	very high	123
19	21.4	557	33	1.2	345	5	215	20	17.3	avg-low	137
20	20.1	562	19	1.6	15	22	185	20	11		130
21	31.8	556	39	1.3	35	20	120	5	22.3	avg	157
22	28	560	40	1.1	130	14	190	15	26.6	avg	164
23	20	555	33	1.2	25	6	250	25	31.6	avg- high	99
24	22.8	550	35	1	225	12	178	30	46	avg	117
25	14.8	563	15.5	1	15	5	270	3	18.6	low	67
26	15	561	21	1.3	10	6	250	3	6.6	avg	74
27	26	561	30	1.2	20	8	180	20	18.6	low	141
28	24.4	552	39	1.1	145	5	175	12	18.3	avg	174
29	25.5	551	32	1	70	5	150	15	30	avg- high	122
30	20.4	556	29	1.2	115	3	310	12	22.3	avg- low	79

Figure 8. Multiple tilting black spruce trees atop a tensionally created mass-movement block; note the correcting posture of the larger tree at right center and the 2–5-year-old sapling, which is growing vertically (just right of the crack edge).

to very-fine (9 micron) polishing sanding film. Sanding and polishing allowed direct observation of individual cells and interpretations of ring boundaries and reaction wood (fig. 7).

SKELETON PLOTTING AND CHRONOLOGY DEVELOPMENT

Once all cores were mounted and sanded, they were dot-counted to allocate a growth year to each ring and then skeleton plotted (Schweingruber and others, 1990). Based on the poor quality of wood from samples 09a, 09b (tree NWJ09), 13a, and 30b, these samples were removed from the dataset. For the remaining 56 samples (representing 29 trees) we used the modified skeleton plot developed by Shroder (1978) to manage our visual-growth analysis (Fantucci, 1999), leading to an event-response graph focused on reaction-wood formation. A reaction-wood response was only recorded if 50 percent or more of the ring consisted of reaction-wood cells, which resulted in a distinctly darker coloration (Stoffel and Corona, 2014) (fig. 7).

Subsequent to dot counting and modified skeleton plotting, ring widths were measured to the nearest 0.001 mm using a Velmex measuring system. The resulting ring-width series (n=56) was processed with COFECHA (Holmes, 1983) to quality assess and quality control the samples for replication/correlation. The resulting data (or series) were standardized (detrended) using ARSTAN version 44h2 (Cook, 2013) to remove biological factors such as the age-related growth trend. Conservative detrending methods were used to maximize low-frequency signals (for example, Cook, 1985).

RESULTS/INTERPRETATIONS

From the 29 trees analyzed (56 cores), the span of time covered (chronology) for these tilted specimens was 175 years (1840–2014; series intercorrelation 0.578). Tilt angles ranged from 3° to 30° for trees with a mean height of 20.8 m (table 1; fig. 9). The averages of thaw depths (TD) as of June 1, 2014, ranged from 6.6 to 73.3 cm (mean 24 cm; table 1). Spearman's rank correlation (rs) of recorded parameters (such as tilt angle, height, age, TD) were calculated at 99 percent and resulted in multiple positive relationships: (a) tree height and diameter at breast height (highest correlation: taller with larger), (b) tree height and age (taller with older), and (c) tilting angle and average TD (more tilted with deeper TD); and one negative relationship: (a) height of tree and tilting angle (taller with less tilted).

We recognized reaction wood in 86 percent of the trees sampled (25 of 29), accounting for 55 percent of all samples (31 of 56 samples). Although expectations were that only the "a" or tilted-side sample would show reaction wood, 21 percent of samples with reaction wood were "b" cores (samples collected at a right angle to the "a" sample), suggesting that more than 21 percent of the trees had been previously tilted (Shroder, 1978, fig. 3). Because of the paucity of reaction wood recorded before 1900 (<<1 percent of samples) our reaction-wood analy-

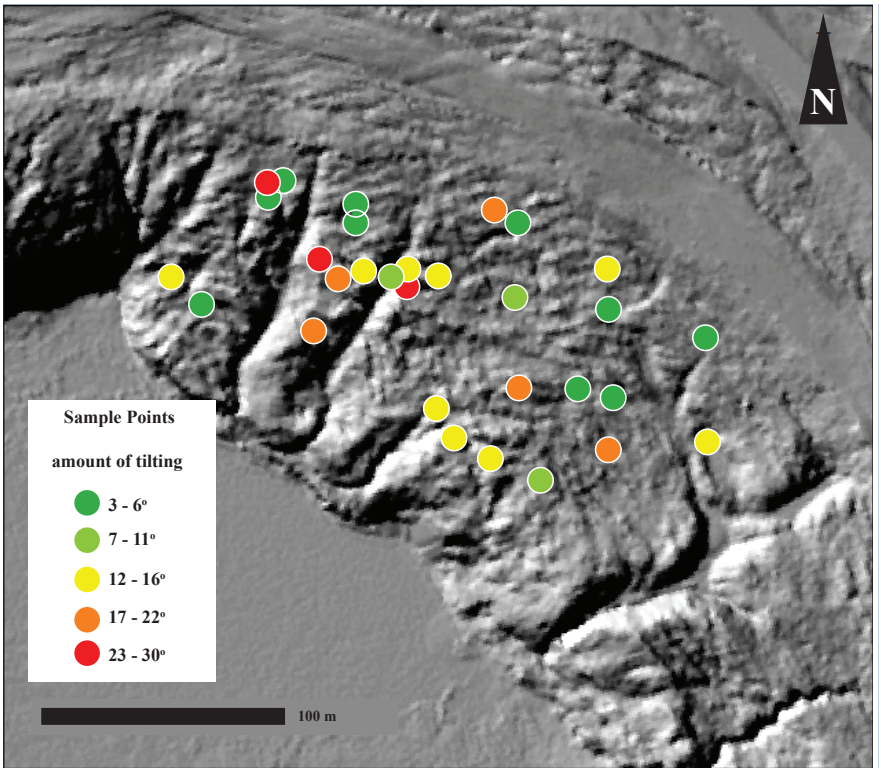

Figure 9. Lidar image of the study site with tree tilts denoted by colored dots.

sis focuses on the past century (1900–2014 = 1899–2013 tilting events) where 12.7 percent of all growth recorded was reaction wood (fig. 10). Decadal and annual statistical analysis of these 115 years reveals a significant increase in reaction-wood abundance starting at the end of the 1980s (figs. 11 and 12). Additional visual analysis of the event-response diagram (fig. 10) also confirms this division beginning in 1989. In the 88 years before 1989, all reaction wood accounted for only 5 percent of recorded tree growth (mean of 2 percent per annum; maximum of 11 percent in 1985); however, from 1989 on, reaction wood accounted for 35 percent of recorded tree growth (mean 10.7 percent per annum; maximum 57 percent in 2012 and 2013). Based on our working assumption that tilting events result in reaction-wood growth within one year of tilting (Cremer, 1998), all sampled trees should have grown reaction-wood since sampling (2014 growth year or beyond), which would increase our maximum reaction wood to 100 percent of sampled trees for 2014 (growth season, post-sampling).

Spatial evaluation of select reaction-wood years, based on hypothesized previous-year tilting (1966, 1989, 1995, 2006, and 2011; fig. 13), reveals site-wide disturbances during each event with a slight weighting to the western side of the site (> 55 percent; for example, 2006). Tilting angles were generally more severe in this western section (n = 16), with an average tilt angle of 13.4° (σ = 8.1°) compared to 11.2° (σ = 5.6°) in the eastern section (n = 13). Analysis of tilt angle and average thaw depth (as of June 1, 2014) results in a positive Spearman's correlation of greater tilt angles associated with deeper thaw depths (fig. 14). This relationship is likely the result of deeper thawing (or localized thaw sinks) leading to strength degradation, which can prime or exacerbate the failure of the landscape (McColl, 2015). This deeper thaw, combined with disrupted sediments from the tensional spread of the mass-movement event and subsequent tree tilting, sediment dilation, and/or tree throw, can lead to increased surface area for thawing processes, leading to a landscape highly susceptible to failure (Benninghoff, 1952; McColl, 2015) (fig. 8).

Chronological and spatial analyses of all measured variables point toward an overall initiation of reaction-wood growth starting in the 1989 growth year as a result of tree tilting in the 1988 growth/non-growth season or the pre-growth season of 1989. This tree-tilting event is likely related to a non-growth timed (or late growth; for example, August 1988 to June 1989; Oswalt, 1960), retrogressive, mass-movement event of complex, spreading blocks of thawing perennially frozen silt (Cruden and Varnes, 1996; Reger and others, 2012a) and not the result of changes only to the site's permafrost, which results in random timing of tilting events (compare to Shroder, 1978). This non-growth timing is also evident

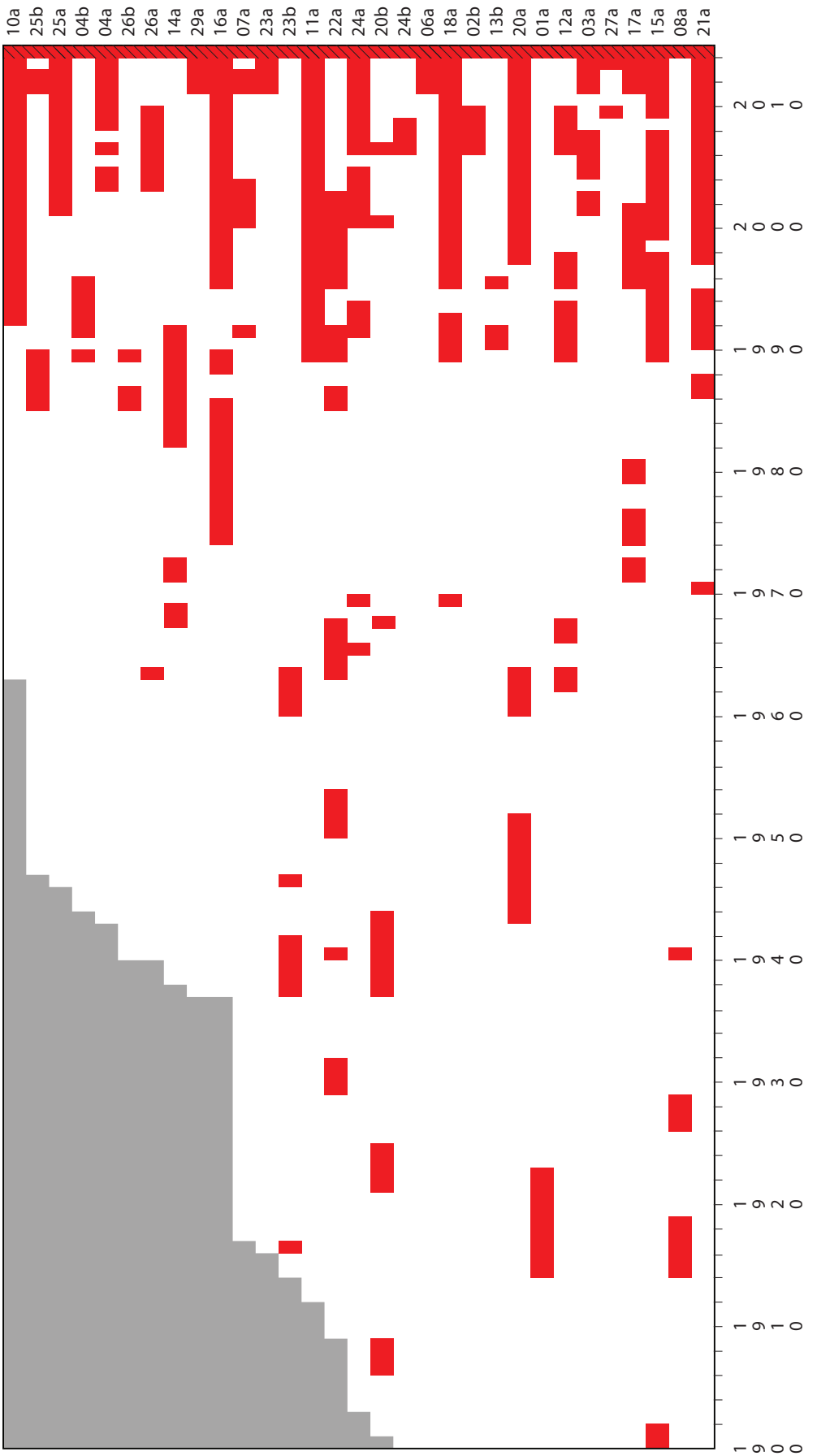

Figure 10. Event-response graph, showing reaction-wood growth by year for 31 samples (1900–2013-14). Red represents recorded reaction wood; the 2014 year is marked with diagonal hachures denoting projected reaction wood because all trees were tilted. Gray represents time not covered by particular samples (for example, the first sample, 10a, was first recorded in 1963).

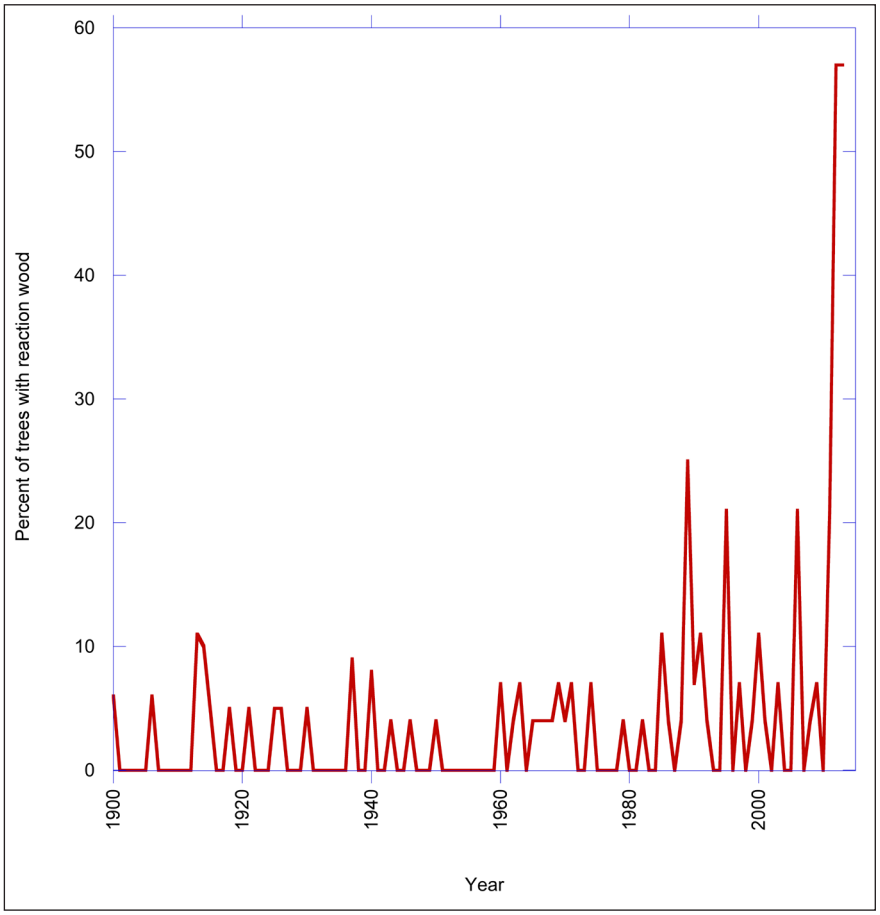

Figure 11. Annual event index, showing the percentage of trees with reaction wood recorded each year. Note the significant increase in abundance around 1990.

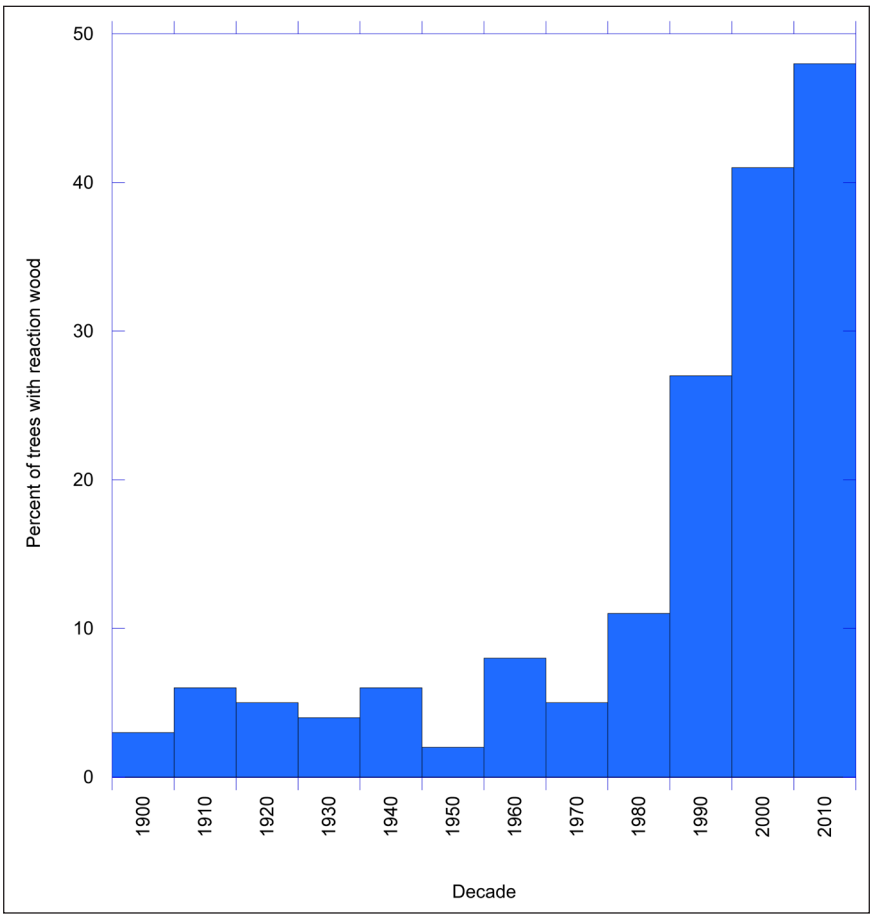

Figure 12. Decadal event index, showing the percentage of trees with reaction wood. Note the significant increase in abundance starting in the 1990s.

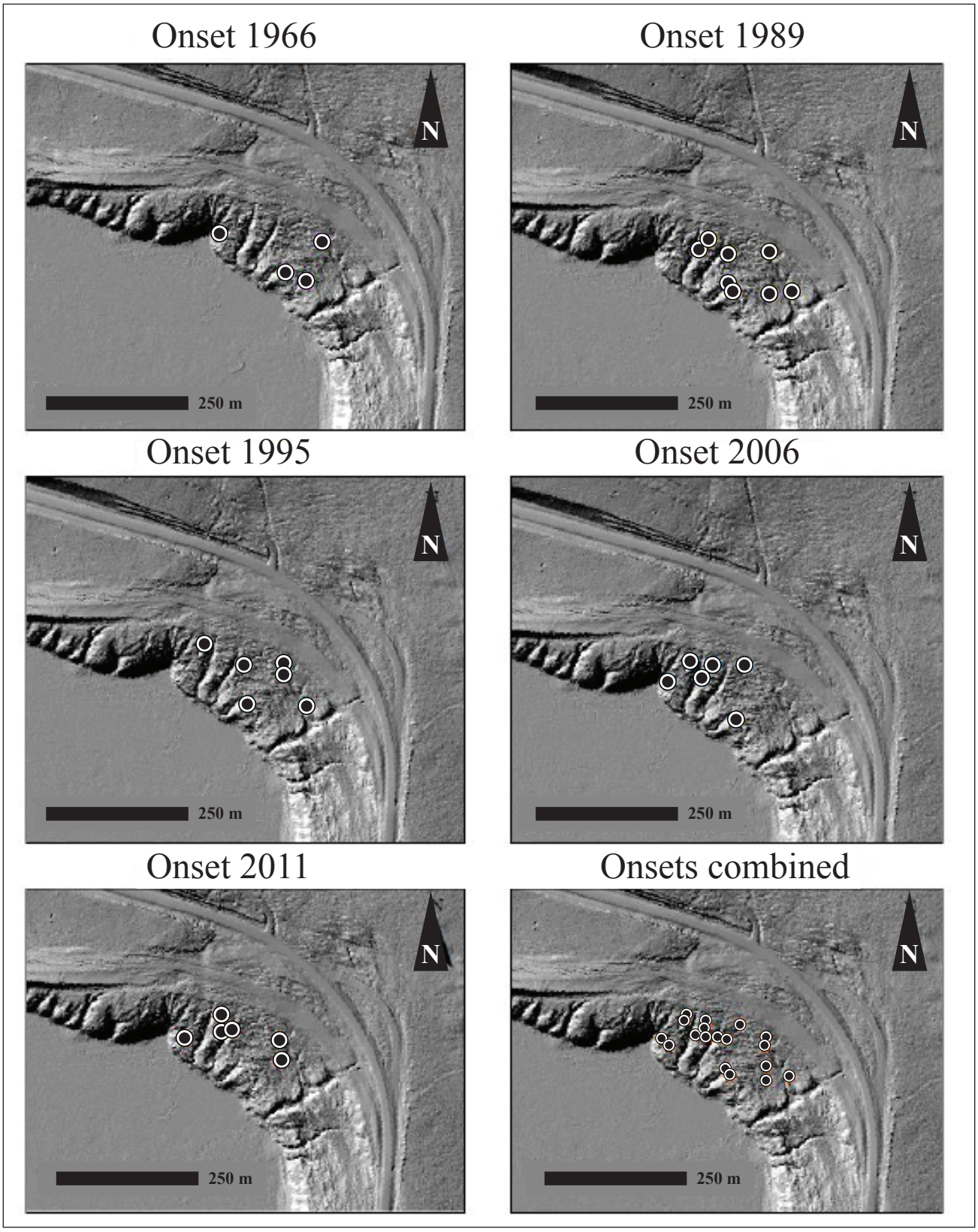

Figure 13. Series of onset maps, which represent dates of reaction wood occurrence in samples based on the working assumption that reaction wood occurs within a year of tilting event (for example, 1989 reaction wood recorded represents a 1988 tilting event). Note the overall distributions of onset are, more or less, site-wide.

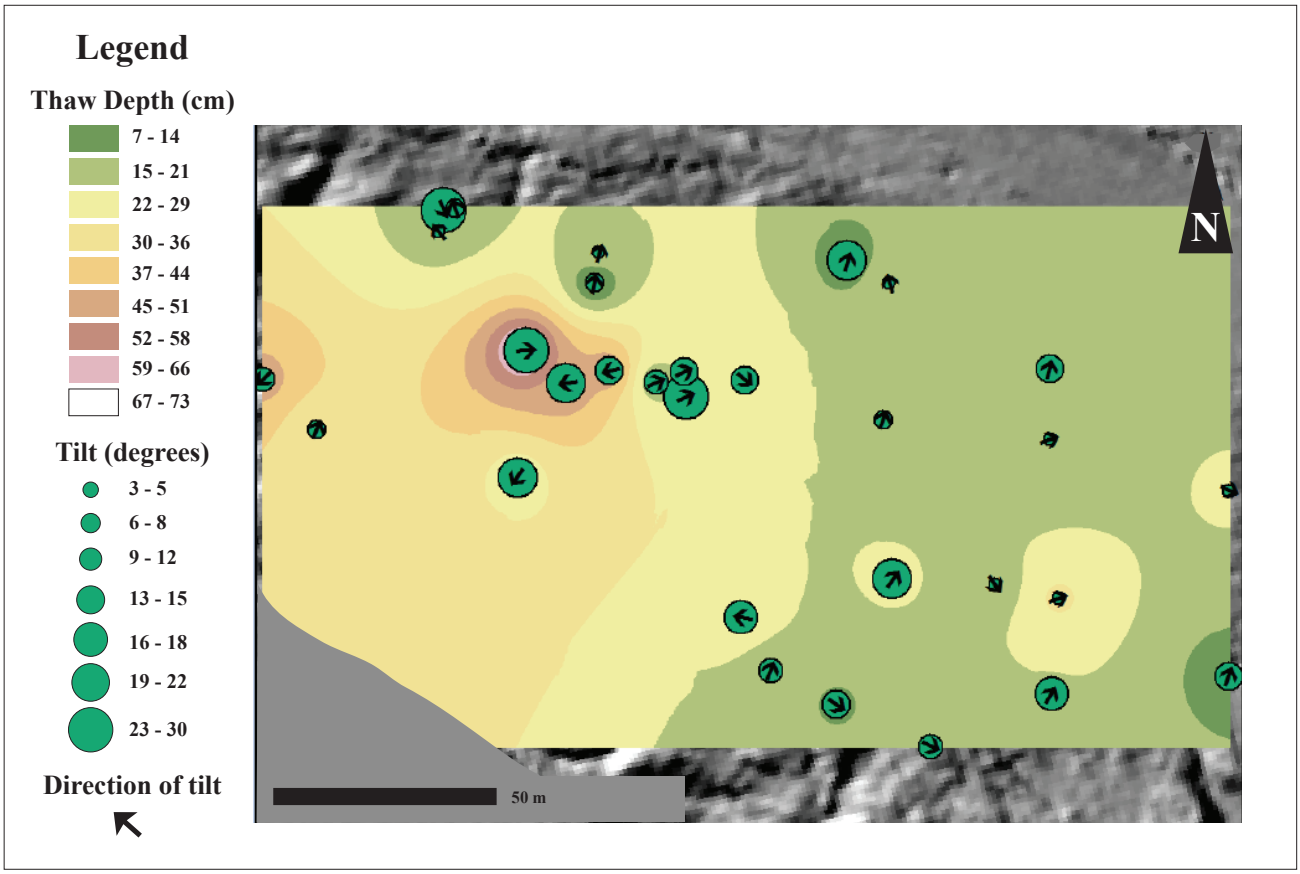

Figure 14. Site map with the spatially analyzed relationship between thaw depth (as of June 10, 2014) and tree-tilt angle. Notice that, generally, the deeper the thaw depth, the more tilted the tree.

in the overall response of the apical meristem, which responds by righting itself within a few days during growth season (Cremer, 1998); 69 percent (n=18) of trees sketched at the appropriate scale show no apical correction, while 31 percent do show apical correction, suggesting latest/earliest growth timing. The direct mechanism for the tilting of these trees as a result of mass movement is likely the deepening of the active layer in permafrost, because trees growing on top of permanently frozen ground have limited anchoring, less flexible rooting (Pulling, 1918), and their roots are encased in ice for most of the year (Benninghoff, 1952). The introduction of tensional cracks breaks up the thermally insulating moss carpet, leading to increased thaw. Increased thaw likely causes decasing of anchored tree-root systems, leading to instability and tilting. These factors become a positive-feedback mechanism, which reduces canopy shading and increases air circulation, leading to more thaw (Benninghoff, 1952; Dingman and Koutz, 1974). Based on this sequence, we believe that this section of ground on which the Alaska Highway is built was mostly stable from at least 1899 until 1987, with no recognized failure associated with the 1942 construction of the highway. In the late-growth or post-growth season of 1988–1989, a sitewide mass-movement event destabilized the site, with continued, significant (re)mobilizations inferred in 1994, 2005, 2010, and, by extension, 2013 (figs. 10 and 13).

CONCLUSIONS

With changing climate impacting higher latitudes at faster rates than lower latitudes (for example, Larsen and others, 2008; D'Arrigo and others, 2014), Alaskans can expect to experience more climate-related changes than their conterminous colleagues (Larsen and others, 2008). Specifically, climate-change effects on all Alaska infrastructure, depending on climate model and implemented adaptations, could add $3.6–6.1 billion in maintenance costs by 2030 and up to $7.6 billion by 2080 (Larsen and others, 2008). A cursory look at the mean annual temperature for Northway (1950-2013) reveals a 3.6-degree Fahrenheit increase in mean-annual temperature, which, is likely a factor in mass movements (Figure 15). In support of risk-based evaluation

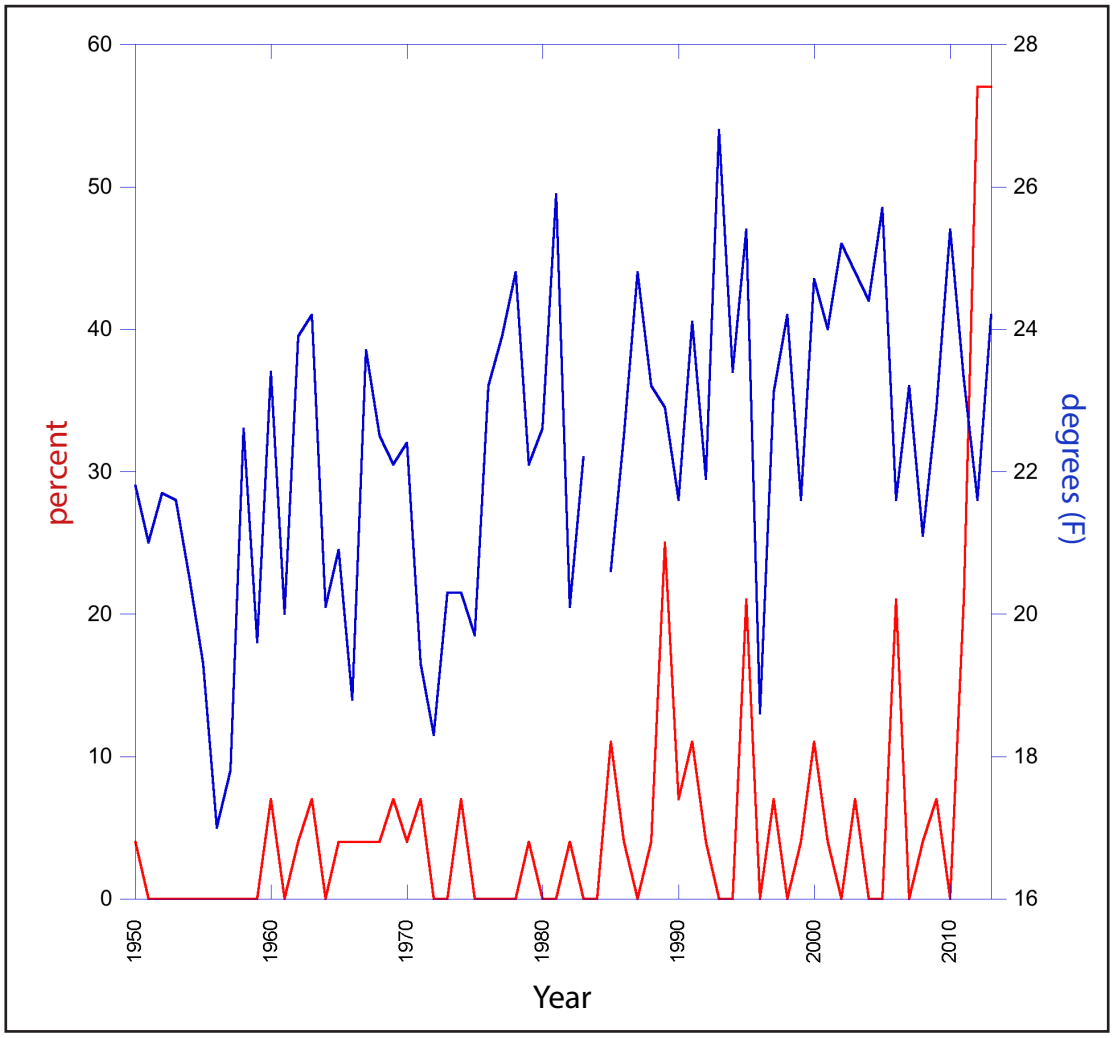

Figure 15. Mean annual temperature graph (blue line) versus percent reaction wood (red line) for the Northway (PAOR) Surface Weather Observation Station (1950-2013).

of infrastructure, DGGS and the Alaska Department of Transportation and Public Facilities (ADOT&PF) have been inspecting and evaluating particular "hot spots" with respect to mass movement to prepare for these eventual changes. At Northway Junction (AMP 1267) an extensional mass-movement site has required multiple repair projects (fig. 2) and a highway realignment in 2004 as a result of the onset of mass movement sometime between about September 1988 and June 1989. Since this time, the approximately 4-hectare site has undergone more-or-less sitewide failure, with significant (re)mobilizations recorded in 1994, 2005, 2010 and, by extension, 2013. It is clear that as this site continues to extend retrogressively and extensionally, increased tensional cracking will allow increased permafrost thawing, leading to decreased site stability over time. Although the 2004 realignment was necessary and engineered well considering the surrounding geology and the particular site, it is only a matter of time before additional large-scale efforts will be required to maintain this section of the Alaska Highway into the next decades.

ACKNOWLEDGMENTS

This work was the result of an undergraduate project, which culminated in a senior thesis completed by Catherine Heinrich in the Department of Geology, St. Lawrence University, in 2015. We thank the project sponsors: the Alaska Division of Geological & Geophysical Surveys (through a Capital Improvement Project), Northway Native Corporation, and the Daniel F. ('65) and Ann H. Sullivan Endowment for Student/Faculty Research University Fellowship and the James Street Fund, both from St. Lawrence University. We also thank Dr. John 'Jack' Shroder (University of Nebraska, Omaha) and Dr. Ronald Daanen (DGGS) for helpful comments and review.

REFERENCES

Alestalo, Jouka, 1971, Dendrochronological interpretation of geomorphic processes: Fennia, v. 105, no. 1, p. 1–140. http://fennia.journal.fi/article/view/40757

Bennett, J.D., 1994, Geotechnical Report, Alaska Highway 1222 North: Alaska Department of Transportation & Public Facilities, Northern Region Technical Services Geology, Federal Project No. IM-0A1-1(9), 230 p.

Benninghoff, W.S., 1950, Use of aerial photographs in mapping vegetation and surficial geology in subarctic regions: Photogrammetric Engineering, v. 16, p. 428–429.

Benninghoff, W.S., 1952, Interaction of vegetation and soil frost phenomena: Arctic, v. 5, no. 1, p. 33–44. http://doi.org/10.14430/arctic3898

Bowman, E.T., 2015, Small landslides—frequent, costly and manageable, *in* Davies, T., ed., Landslide hazards, risks and disasters: Amsterdam, Elsevier, p. 405–439, http://doi.org/10.1016/B978-0-12-396452-6.00012-4

Brazo, G.M., 1984, Engineering geology and soils report, Alaska Highway miles 1256 to 1270: Alaska Department of Transportation & Public Facilities, Northern Region Design and Construction, Project Number IR-I-0A1-1(3), (4), 86 p.

Carrara, P.E., 2002, Response of Douglas firs along the fault scarp of the 1959 Hebgen Lake earthquake, southwestern Montana: Northwest Geology, v. 31, p. 54–65.

Carrara, P.E., and O'Neill, J.M., 2010, Tree-ring dated landslide movements and seismic events, *in* Stoffel, Markus, Bollschweiler, Michelle, Butler, D.R., and Luckman, B.H., eds., Tree rings and natural hazards—A state-of-the-art: Dordrecht, Netherlands, Springer, p. 421–436.

CEC (Commission for Environmental Cooperation), 1997, Ecological regions of North America—Toward a common perspective: Montreal, QC, Canada, Commission for Environmental Cooperation. http://www3.cec.org/islandora/en, last accessed July 2016.

Chapin, F.S., III, McGuire, A.D., Ruess, R.W., Hollingsworth, T.N., Mack, M.C., Johnstone, J.F., Kasischke, E.S., Eus-kirchen, E.S., Jones, J.B., Jorgenson, M.T., Kielland, K., Kofinas, G.P., Turetsky, M.R., Yarie, J., Lloyd, A.H., and Taylor, D., 2010, Resilience of Alaska's boreal forest to climatic change: Canadian Journal of Forest Research, v. 40, no. 7, p. 1,360–1,370. http://doi.org/10.1139/X10-074

CLIMOD, 2016, Northway Airport weather station (PAOR), 1942–present: http://climodtest.nrcc.cornell.edu, last accessed July 2016.

Cook, E.R., 1985, A time series analysis approach to tree-ring standardization: Tucson, University of Arizona, Ph.D. dissertation, 183 p.

Cook, E.R., 2013, ARSTAN, chronology development and analysis software, version 44h2—Available from Lamont-Doherty Earth Observatory, http://www.ldeo.columbia.edu/tree-ring-laboratory/resources/software, last accessed July 2016.

Cremer, K.W., 1998, Recovery of Pinus radiata saplings from tilting and bending: Australian Forestry, v. 61, no. 3, p. 211–219. http://doi.org/10.1080/00049158.1998.10674743

Cruden, D.M., and Varnes, D.J., 1996, Landslide types and processes; Chapter 3, *in* Turner, A.K., and Schuster, R.L., eds., Landslides—Investigations and mitigation: Washington DC, Transportation Research Board, National Research Council, Special Report 247, p. 36–75.

D'Arrigo, Rosanne, Davi, Nicole, Jacoby, Gordon, Wilson, Rob, and Wiles, Greg, 2014, Dendroclimatic studies—Tree growth and climate change in northern forests: American Geophysical Union, Wiley Press, Special Publications Series, 88 p.

Dingman, S.L., and Koutz, F.R., 1974, Relations among vegetation, permafrost, and potential insolation in central Alaska: Arctic and Alpine Research, v. 6, no. 1, p. 37–42. http://doi.org/10.2307/1550368

DoD (Department of Defense), 1944, Alaska Highway: U.S. War Department Official Film, misc. 959, https://archive.org/details/gov.dod.dimoc.23086#maincontent, last accessed July 2016.

Fantucci, Rosanna, 1999, Dendrogeomorphology in landslide analysis Casale, R., and Margottini, C., eds., Floods and landslides—Integrated risk assessment: Berlin, Springer, Environmental Science series, p. 69–81.

Fantucci, Rosanna, and McCord, A., 1995, Reconstruction of landslide dynamic with dendrochronological methods: Dendrochronologia, v. 13, p. 43–58.

Fritts, Harold C., 1976, Tree rings and climate: New York, Academic Press, 567 p.

Fryer, Janet L., 2014a, Picea mariana, Fire effects information system [online]: U.S. Department of Agriculture, Forest Service, Rocky Mountain Research Station, Fire Sciences Laboratory (producer). http://www.fs.fed.us/database/feis/plants/tree/picmar/all.html, last accessed July 2016.

Fryer, Janet L., 2014b, Fire regimes of Alaskan black

spruce communities, *in* Fire effects information system [online]: U.S. Department of Agriculture, Forest Service, Rocky Mountain Research Station, Fire Sciences Laboratory (producer). http://www.fs.fed.us/database/feis/fire_regimes/AK_black_spruce/all.html, last accessed July 2016.

Gallant, A.L., Binnian, E.F., Omernik, J.M., Shasby, M.B., 1995, Ecoregions of Alaska: U.S. Geological Survey Professional Paper 1567, 73 p., 1 plate. https://pubs.er.usgs.gov/publication/pp1567, last accessed July 2016.

Hogg, E.H., 1994, Climate and the southern limit of the western Canadian boreal forest: Canadian Journal of Forest Research, v. 24, no. 9, p. 1,835–1,845. http://doi.org/10.1139/x94-237

Holmes, R.L., 1983, Computer-assisted quality control in tree-ring dating and measurement: Tree-Ring Bulletin, v. 43, p. 69–78.

Hubbard, T.D., Braun, M.L., Westbrook, R.E. and Gallagher, P.E., 2011, High-resolution lidar data for infrastructure corridors, Tanacross Quadrangle, Alaska, *in* Hubbard, T.D., Koehler, R.D. and Combellick, R.A., High-resolution lidar data for Alaska infrastructure corridors: Alaska Division of Geological & Geophysical Surveys Raw Data File 2011-3B. http://doi.org/10.14509/22724

Jorgenson, M.T., Racine, C.H., Walters, J.C., and Osterkamp, T.E., 2001, Permafrost degradation and ecological changes associated with a warming climate in central Alaska: Climatic Change, v. 48, p. 551–579.

Jorgenson, M.T., Yoshikawa, Kenji, Romanovsky, Vladimir, Kanevskiy, Mikhail, Brown, Jerry, Shur, Yuri, Marchenko, Sergei, Grosse, Guido, and Jones, Ben, 2008, Permafrost characteristics of Alaska [abstr.], *in* Kane, D.L., and Hinkel, K.M., eds., Extended Abstracts, Ninth International Conference on Permafrost, Fairbanks, Alaska, June 29–July 3, 2008: University of Alaska Fairbanks Institute of Northern Engineering, v. I, p. 121–122.

Kinney, T.C., 1993, Geotechnical report, Alaska Highway M.P. 1268 slide: Fairbanks, AK, Shannon & Wilson, Inc., Geotechnical and Environmental Consultants, Federal Project No. IR-0A1-1(8), 44 p.

Larsen, P.H., Goldsmith, Scott, Smith, Orson, Wilson, M.L., Strzepek, Ken, Chinowsky, Paul, and Saylor, Ben, 2008, Estimating future costs for Alaska public infrastructure at risk from climate change: Global Environmental Change, v. 18, no. 3, p. 442–457, http://doi.org/10.1016/j.gloenvcha.2008.03.005

Mattheck, Claus, 1993, Design in der Natur—der Baum als Lehrmeister: Freiburg, Rombach, 242 p.

McColl, S.T., 2015, Landslide causes and triggers Davies, T., ed., Landslide hazards, risks and disasters: Amsterdam, Elsevier, p. 17–42. http://doi.org/10.1016/B978-0-12-396452-6.00002-1

Oswalt, W.H., 1960, The growing season of Alaskan spruce: Tree-Ring Bulletin, v. 23, p. 3–9.

Owczarek, Piotr, 2005, Dendrochronological dating of geomorphic processes in the High Arctic: Landform Analysis, v. 14, p. 45–56. http://www.sgp.org.pl/la/lav14.htm

Pastick, N.J., Jorgenson, M.T., Wylie, B.K., Rose, J.R., Rigge, M. and Walvoord, M.A., 2014, Spatial variability and landscape controls of near-surface permafrost within the Alaskan Yukon River Basin: Journal of Geophysical Research, Biogeosciences, v. 119, p. 1,244–1,265. http://doi.org/10.1002/2013JG002594

Pastick, N.J., Jorgenson, M.T., Wylie, B.K., Nield, S.J., Johnson, K.D. and Finley, A.O., 2015, Distribution of near-surface permafrost in Alaska—Estimates of present and future conditions: Remote Sensing of the Environment, v. 168, p. 301–315. http://doi.org/10.1016/j.rse.2015.07.019

Pulling, H.E., 1918, Root habit and plant distribution in the far north: Plant World, v. 21, p. 223–233. http://www.jstor.org/stable/43477713

Reger, R.D., Hubbard, T.D., and Gallagher, P.E., 2012a, Reconnaissance interpretation of 1978–1981 permafrost, Alaska Highway corridor, Tetlin Junction to Canada border, Alaska: Alaska Division of Geological & Geophysical Surveys Preliminary Interpretive Report 2012-1C, 27 p., 2 sheets, scale 1:63,360. http://doi.org/10.14509/23444

Reger, R.D., Hubbard, T.D., and Gallagher, P.E., 2012b, Surficial geology of the Alaska Highway corridor, Tetlin Junction to Canada border, Alaska: Alaska Division of Geological & Geophysical Surveys Preliminary Interpretive Report 2012-1A, 25 p., 2 sheets, scale 1:63,360. http://doi.org/10.14509/23443

Reger, R.D., Hubbard, T.D., and Koehler, R.D., 2017, Surficial geology and geohazards in the Alaska Highway corridor, Alaska: Alaska Division of Geological & Geophysical Surveys Report of Investigation 2017-1, *in press*. http://doi.org/10.14509/29701

Schaefer, J.R.G., 2002, Stratigraphy, major oxide geochemistry, and $^{40}Ar/^{39}Ar$ geochronology of a tephra section near Tok, Alaska: Fairbanks, University of Alaska Fairbanks M.S. thesis, 62 p.

Schweingruber, F.H., Eckstein, D., Serre-Bachet, F., and Bräker, O.U., 1990, Identification, preservation, and interpretation of event years and pointer years

in dendrochronology: Dendrochronologia, v. 8, p. 9–38.

Shroder, J.F., Jr., 1978, Dendrogeomorphological analysis of mass movement on Table Cliffs Plateau, Utah: Quaternary Research, v. 9, no. 2, p. 168–185. http://doi.org/10.1016/0033-5894(78)90065-0

Shur, Y.L. and Jorgenson, M.T., 2007, Patterns of permafrost formation and degradation in relation to climate and ecosystems: Permafrost and Periglacial Processes, v. 18, no. 1, p. 7–19. http://doi.org/10.1002/ppp.582

Solie, D.N., Werdon, M.B., Freeman, L.K., Newberry, R.J., Szumigala, D.J., Speeter, G.G., Elliott, B.A., *in press*, Bedrock geologic map, Alaska Highway corridor, Tetlin Junction to Canada border: Alaska Division of Geological & Geophysical Surveys Report of Investigation, 2 map sheets, scale 1:63,360.

Speer, J.H., 2010, Fundamentals of tree-ring research: Tucson, The University of Arizona Press, 368 p.

Stoffel, Markus, and Corona, Christophe, 2014, Dendroecological dating of geomorphic disturbance in trees: Tree-Ring Research, v. 70, no. 1, p. 3–20. http://doi.org/10.3959/1536-1098-70.1.3

Stoffel, Markus, Bollschweiler, Michelle, Butler, D.R., and Luckman, B.H., 2010, Tree rings and natural hazards—A state-of-the-art: Dordrecht, Netherlands, Springer, 505 p.

Stoffel, Markus, Butler, D.R. and Corona, Christophe, 2013, Mass movements and tree rings—A guide to dendrogeomorphic field sampling and dating: Geomorphology, v. 200, p. 106–120. http://doi.org/10.1016/j.geomorph.2012.12.017

Viereck, L.A., and Johnston, W.F., 1990, Silvics of North America, Volume 1, Confers—Picea mariana (Mill.) B.S.P.: U.S. Forest Service, v. 1. http://www.na.fs.fed.us/spfo/pubs/silvics_manual/table_of_contents.htm, last accessed July 2016.

Wahrhaftig, Clyde, 1965, Physiographic divisions of Alaska: U.S. Geological Survey Professional Paper 482, 52 p. http://pubs.er.usgs.gov/publication/pp482, last accessed July 2016.

Wallace, R.E., 1948, Cave-in lakes in the Nabesna, Chisana, and Tanana river valleys, eastern Alaska: Journal of Geology, v. 56, no. 3, p. 171–181. http://doi.org/10.1086/625498

Warensjö, Mats, and Rune, Göran, 2004, Stem straightness and compression wood in 22-year-old stand of container-grown Scots pine trees: Silva Fennica, v. 38, no. 2, article 424, p. 143–153. http://doi.org/10.14214/sf.424

Westing, A.H., 1965, Formation and function of compression wood in gymnosperms: Botanical Review, v. 31, no. 3, p. 381–480. http://doi.org/10.1007/BF02859131

Wiken, Ed, Nava, F.J., and Griffith, Glenn, 2011, North American terrestrial ecoregions—Level III: Montreal, Canada, Commission for Environmental Cooperation (CEC), 149 p. http://www3.cec.org/islandora, last accessed July 2016.

Wilson, F.H., Hults, C.P., Mull, C.G., and Karl, S.M., comps., 2015, Geological map of Alaska: U.S. Geological Survey Scientific Investigations Map 3340, 197 p., 2 sheets, scale 1:584,000. http://doi.org/10.3133/sim3340